Investigations on copper chloride doped polyaniline composites as efficient electrode materials for supercapacitor applications

Saptarshi Dhibar · Sumanta Sahoo ·
C. K. Das · R. Singh

Abstract In this study, we have discussed the potential of using copper chloride (CuCl$_2$) doped Polyaniline (PANI) as an electrode material for supercapacitor application. PANI in pure and doped forms with various doping levels of CuCl$_2$ (doping levels of 1, 2, 3 and 4 wt%) were synthesized by in situ polymerization method, using ammonium peroxodisulfate as oxidant in HCl medium. The morphology of the doped polymeric materials was studied by scanning electron microscope and transmission electron microscope analysis. The interaction between PANI and the metal cation (Cu^{2+}) was confirmed by the fourier transform infrared spectroscopy analysis. Thermal stability of the materials was examined by thermogravimetric analysis. Electrochemical characterizations of the materials were carried out by three electrode probe method where, platinum and saturated standard calomel electrode were used as counter and reference electrode respectively. 1 M KCl solution was used as electrolyte for all the electrochemical characterizations. Among all the materials, PANI shows highest specific capacitance value at the doping level of 2 wt%.

1 Introduction

Over the last decades, a new class of organic polymers has been synthesized with the ability to conduct electric current. These types of polymers are known as conducting polymers. The general aspect of most electrically conducting polymers is the presence of an extended π-conjugation system with single and double bond alteration along the polymer backbone. Conducting polymers are semiconductor materials in nature with low charge carrier mobility [1–5]. Apart from electrical properties, the unique magnetic properties, optical and chemical properties of the conducting polymers have led them to a wide range of technological applications in electromagnetic interference shielding, rechargeable batteries, electrodes, corrosion protection coatings, sensors, and microwave absorption [6–10]. Among the conducting polymers, PANI is one of the smart polymers for its easy synthesis, relatively cheap, high electrical conductivity, exclusive electrochemical properties, and good environmental stability [11–18]. PANI can easily be synthesized through electrochemical or chemical oxidation of aniline with the help of oxidants like ammonium persulfate in acidic medium [19–23].

Supercapacitors, also known as, electrochemical capacitors, have been recognized for over 50 years and are considered as one of the most promising energy storage system in addition to batteries [24–27]. There are two types of electrochemical capacitors based on the type of electrochemical response. The most commonly known capacitors are those, exhibiting high surface reactivity, resulting in the development of double layer, also originally called electric double layer capacitors (EDLC). The second category of capacitor materials are the ones showing Faradic electrochemical reactions occurring on the surface.

Nowadays, PANI doped with metal ions has attracted much more research attention due to its potential applications such as redox-active catalyst [28], corrosion inhibitor [29], etc. Many research articles are available on PANI doped with various metal ions. Ozkazanc et al. [30] reported the synthesis and characterization of PANI both in

S. Dhibar · S. Sahoo · C. K. Das (✉)
Materials Science Centre, Indian Institute of Technology,
Kharagpur 721302, India
e-mail: chapal12@yahoo.co.in

R. Singh
Defence Research and Development Organization, New Delhi,
India

pure and doped forms with various levels of $CuCl_2$ and $ZnCl_2$ in HCl medium and examined the structural and dielectric properties. Gupta et al. [31] synthesized PANIs doped with different dopants like $CuCl_2$ and $CoCl_2$ and measured their magnetic and alternating current transport properties. Yang and Chen [32] reported the synthesis of PANI containing transition metal ions by chemically oxidizing the complex of aniline with transition metal ions such as Fe^+, Co^+, Ni^+ and Cu^+. Rivas and Sancchez [33] investigated the interaction between various metals ions and functional PANI by using PANI derivative and studied their thermal stability, and electrical conductivity. Dimitriev [34] reported the effect of doping of PANI films by transition metal salts and determined their conductivities. He also reported on employment of transition metals salts as conventional chemical agents, which has the capability to interact with PANI chains directly and checked the film morphology, conductivity, and electronic spectra [35]. Gizdavic-Nikolaidis et al. [36] reported the investigation of HCl doping with 0.1 M $CuCl_2$ aqueous solution by spectroscopic methods and the conductivities of the samples were also measured.

However, many researchers are now interested to prepare electrode materials for supercapacitors based on conducting polymers, doped with different metal ions. Li et al. [37] synthesized polyaniline co-doped with Zn^{2+} and H^+ was in aqueous solution containing $ZnCl_2$ by simple chemical polymerization method and found maximum specific capacitance of 369 F/g. Further, Patil et al. [38] reported the Mn doped polyaniline thin films, deposited on stainless steel substrates, prepared by sonochemical method and achieved highest specific capacitance of 474 F/g in 1.0 M H_2SO_4 electrolyte. Ryu et al. [39] investigated the electrochemical performances of asymmetric redox supercapacitor based on $LiPF_6$ and HCl doped polyaniline using chemical methods and observed a maximum specific capacitance of 115 F/g. Palaniappan and Devi [40] successfully prepared dual-acid-doped polyaniline electrode and achieved maximum discharge capacitance of 140 F/g for HBF_4 doped PANI. As a whole, the redoping and dedoping processes in PANI systems plays an important role for their potential application as electrode materials for supercapacitors. But, to the best of our knowledge, till now no literatures are available on the electrochemical performances of Cu^{2+} doped PANI. So our motivations of this study are to synthesize $CuCl_2$ doped PANI and investigate their potential to be used as an electrode material for supercapacitor applications. Our ambition is also to study the effect of different doping levels of PANI on the electrochemical performances. Overall, the main aim of this study is to obtain a new polymeric material with good electrochemical properties.

In this present study, PANI doped with $CuCl_2$ in various doping levels was synthesized by in situ polymerization method, using APS as oxidant in HCl medium. The capacitive behavior of PANI and doped PANI were investigated by cyclic voltammetry (CV) and electrochemical impedance spectroscopy (EIS) analysis. Further, the thermal properties, morphological study as well as chemical interaction in doped samples were also investigated by different characterization techniques.

2 Experimental

2.1 Materials used

The monomer, aniline used in this study was supplied by Merck, Germany. Ammonium persulfate [$(NH_4)_2S_2O_8$] and HCl used in this study were supplied by Merck, Germany. Copper chloride ($CuCl_2$) used in this study was also supplied by Merck, Germany.

2.2 Synthesis of polyaniline

PANI was synthesized by chemical oxidation polymerization where ammonium persulfate [$(NH_4)_2S_2O_8$] was used as oxidant. At first, 2 ml aniline was dissolved in 1.5 M, 70 ml HCl solution in a 200 ml beaker. In another beaker, 4 g of $(NH_4)_2S_2O_8$ dissolved in 20 ml deionized water. This solution was added drop wise to the aniline solution. The whole solution was stirred at constant speed for 5 h at a constant temperature of 25 °C. After the polymerization, the whole solution was filtered, washed with deionized water and ethanol several times, and dried to get green emeraldine salt form of PANI granules.

2.3 Doping process

$CuCl_2$ salt of various doping levels of 1, 2, 3, and 4 wt % each prepared in 5 ml deionized water, was added into the bulk solution prepared (as described in the Sect. "2.2"), just before the stirring stage. The whole solution was again stirred at constant speed and constant temperature of 25 °C for 5 h. After the polymerization, the whole solution was again filtered, washed with deionized water and ethanol several times and dried at 60 °C in order to form doped PANI samples [30]. The compositions of the composites are summarized in Table 1.

3 Characterization

3.1 FTIR analysis

FTIR was performed using NEXUS 870 FT-IR (Thermo Nicolet) instrument in the range from 4,000 to 400 cm^{-1}.

Table 1 Composition of the composites

Sample codes	CuCl$_2$ (wt %)	Polyaniline (wt %)
PANI	0	100
PANI C1	1	99
PANI C2	2	98
PANI C3	3	97
PANI C4	4	96

The samples were prepared by mixing potassium bromide (KBr) and polyaniline composites in weight ratio of 10:1 and pelletized to make the disk and the disk was analyzed for getting the spectrum.

3.2 Surface morphology study

A scanning electron microscope (SEM, VEGA II LSU, TESCAN, Czech Republic) was used to study the surface morphology of the polyaniline composites. The powder samples were put on the carbon tap and then sputter coated with gold. SEM micrographs were taken at an operating voltage of 10 kV.

3.3 High resolution transmission electron microscopy (HR-TEM) study

The doped polyaniline composites were analyzed by the high resolution transmission electron microscopy (HR-TEM, JEOL 2100) to check the uniformity of the coating of Cu^{2+} on the polyaniline. A small amount of sample was put in the acetone and sonicated for 30 min in an ultrasonic bath. Then a drop of this dispersed solution was injected on the copper grid for the HR-TEM analysis.

3.4 Electrochemical characterization

Electrochemical analysis such as CV, EIS were carried on GAMRY instrument (750 mA and 1.6 V) by using a three electrode system where platinum and saturated calomel electrode (SCE) were used as counter and reference electrodes respectively. Cyclic voltammetry measurement was performed in 1 M KCl solution at different scan rate from 10 to 200 mV/s. The specific capacitances of the electrode materials were calculated by the following equation [41–43].

$$C_{sp} = (I_+ - I_-)/v \times m \qquad (1)$$

where I_+ and I_- are maximum current in positive and negative voltage scan respectively, v is the scan rate and m is the mass of the composite materials. Impedance measurements were carried out for all the composites in

1 M aqueous KCl solution by EIS. The samples were prepared by pressing the composite materials at 10 MPa pressure. The electrodes were used for electrochemical characterization without any polymer binder.

3.5 Thermal analysis

The thermal stability of the pure PANI and PANI doped with CuCl$_2$ composites were investigated using a thermogravimertic analyzer (TGA 209F, from NETZSCH, Germany). TGA analysis was conducted with a heating rate of 10 °C/min under nitrogen atmosphere.
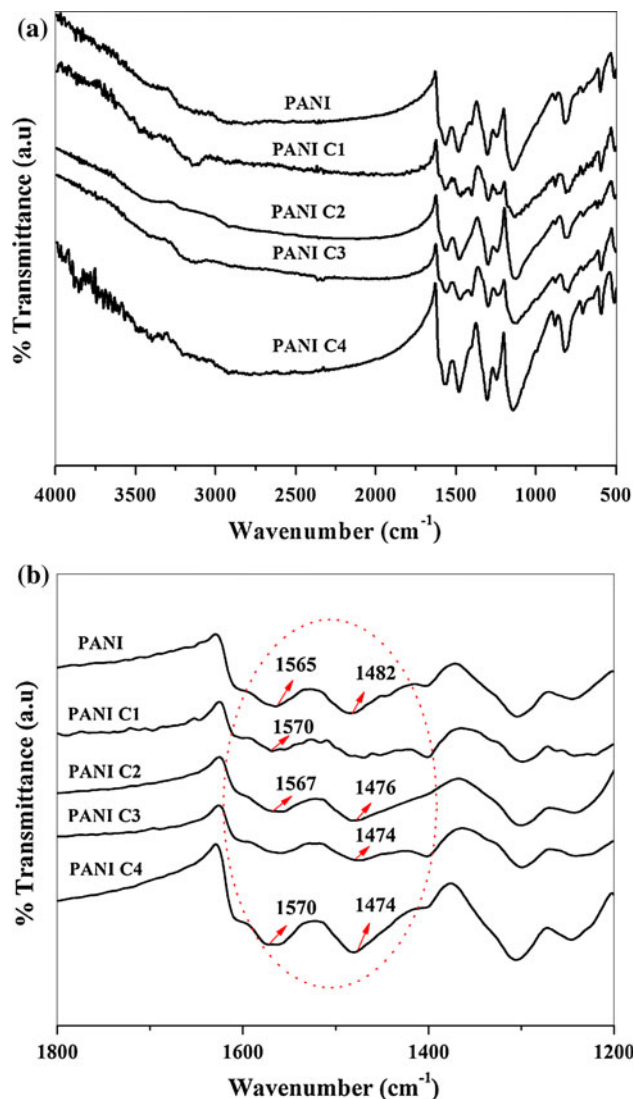

Fig. 1 **a** FTIR spectrum of pure PANI, PANI C1, PANI C2, PANI C3, and PANI C4 composites. **b** Magnified FTIR spectrum

4 Results and discussion

4.1 FTIR analysis

The FTIR spectrum of pure PANI and doped PANI are shown in Fig. 1a. Similar kind of spectrum was observed by Ozkazanc et al. [30]. N–H stretching with weak absorbance is found within the range of 3,500–3,100 cm^{-1}, whereas C–H stretching is found within the range of 3,050–2,800 cm^{-1}. The peaks at 1,565 and 1,482 cm^{-1} are related to quinine and benzene ring stress deformation, respectively. The band characteristics of the emeraldine salt form (or conducting protonated form) are observed at 817, 1144, 1246, and 1305 cm^{-1}. These bands are assigned to the vibration mode of the –NH$^+$= structure, which may be formed during the protonation of imine sites. It is also observed from the spectrum that the quinoid and benzenoid peaks forming the main peaks of the spectrum have shifted upon the addition of Cu^{2+} from 1,482 to 1,474 cm^{-1} and from 1,565 to 1,570 cm^{-1} respectively. The magnified portion of the FTIR spectrum of the composite
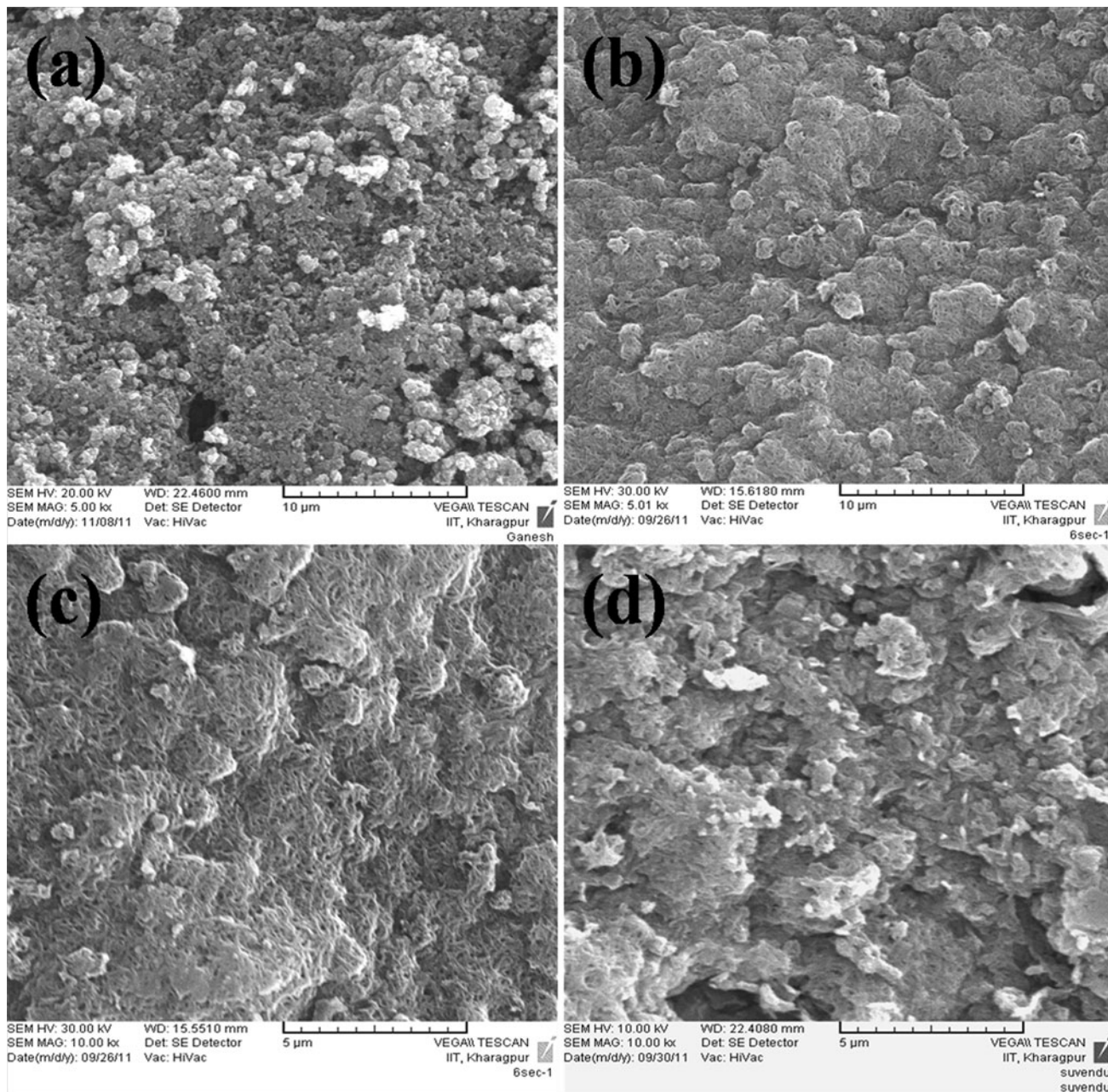

Fig. 2 SEM images of **a** pure PANI, **b** PANI C2 at lower magnification, **c** PANI C2 at higher magnification, and **d** PANI C3 composites

materials clearly shows the shifting of these particular picks (Fig. 1b). This shift arises may be due to the interactions between PANI and the metal cation, Cu^{2+} [30].

4.2 Surface morphology study

Figure 2 represents the SEM images of pure PANI and $CuCl_2$ doped PANI composites. In case of pure PANI, shown in Fig. 2a, we can observe that the grains are well resolved and circular. Figure 2b, c shows the SEM images of $CuCl_2$ doped PANI at 2 wt% doping level at low and high magnification which shows that the grains are converted to fiber like structure. This type of special morphology arises due to better interaction of PANI and Cu^{2+} at 2 wt% doping level. Figure 2d shows similar morphology as that of pure PANI.

4.3 HRTEM analysis

The morphological characteristics of $CuCl_2$ doped PANI was investigated by HRTEM and images are shown in Fig. 3. Figure 3a, b represents the TEM images of PANI doped with $CuCl_2$ at 1 and 2 wt% doping levels. Figure 3a shows doped and undoped PANI. However, uniform doping of PANI by $CuCl_2$ is observed in PANI C2 composite (shown in Fig. 3b). So, we can expect that, due to the uniform doping, capacitance properties of PANI C2 will be better than PANI C1 (discussed in the Sect. "4.4").

4.4 Electrochemical characterization

Cyclic voltammograms of pure PANI and PANI doped with $CuCl_2$ at different doping level are shown in Fig. 4. Their specific capacitances of the electrode materials are summarized in Table 2. Pure PANI and doped composites were analyzed within the applied voltage range of -0.8 to $+0.8$ V. The mass of the active electrode materials were around 12 mg. These types of electrode materials are Pseudocapacitive in nature. Hence, the charge storage mechanism of these electrode materials is of Faradic type. These types of Pseudocapacitors can store charge through charge transfer between electrode and electrolyte. However, among the pure PANI and PANI doped $CuCl_2$ composites, PANI C2 shows maximum specific capacitance of 626 F/g at 10 mV/s scan rate. On the other hand, pure PANI, PANI C1, PANI C3, and PANI C4 shows specific capacitance value of 397, 458, 381, and 439 F/g respectively. However, PANI C3 shows lower specific capacitance than that of pure PANI. This decrease in the specific capacitance can be attributed towards the specific surface area accessible by the electrolyte. The PANI C2 shows higher specific capacitance due to uniform doping of PANI by $CuCl_2$, which is also revealed from the HRTEM studies. Additionally, for all the composites, it is observed that with increase in the scan rate, the specific capacitance values decreases, which is shown in Fig. 5. This may be due to the result of greater charge mobilization per unit time.

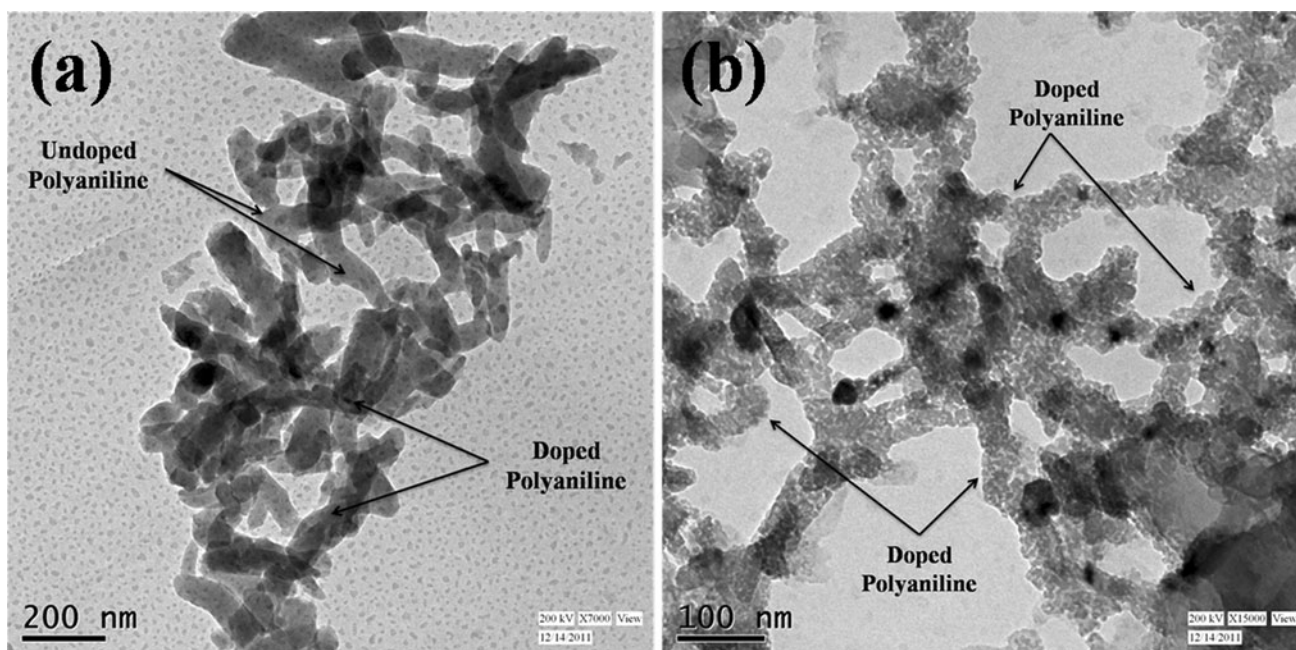The use of supercapacitor also depends on its energy density and power density. The prime disadvantage of

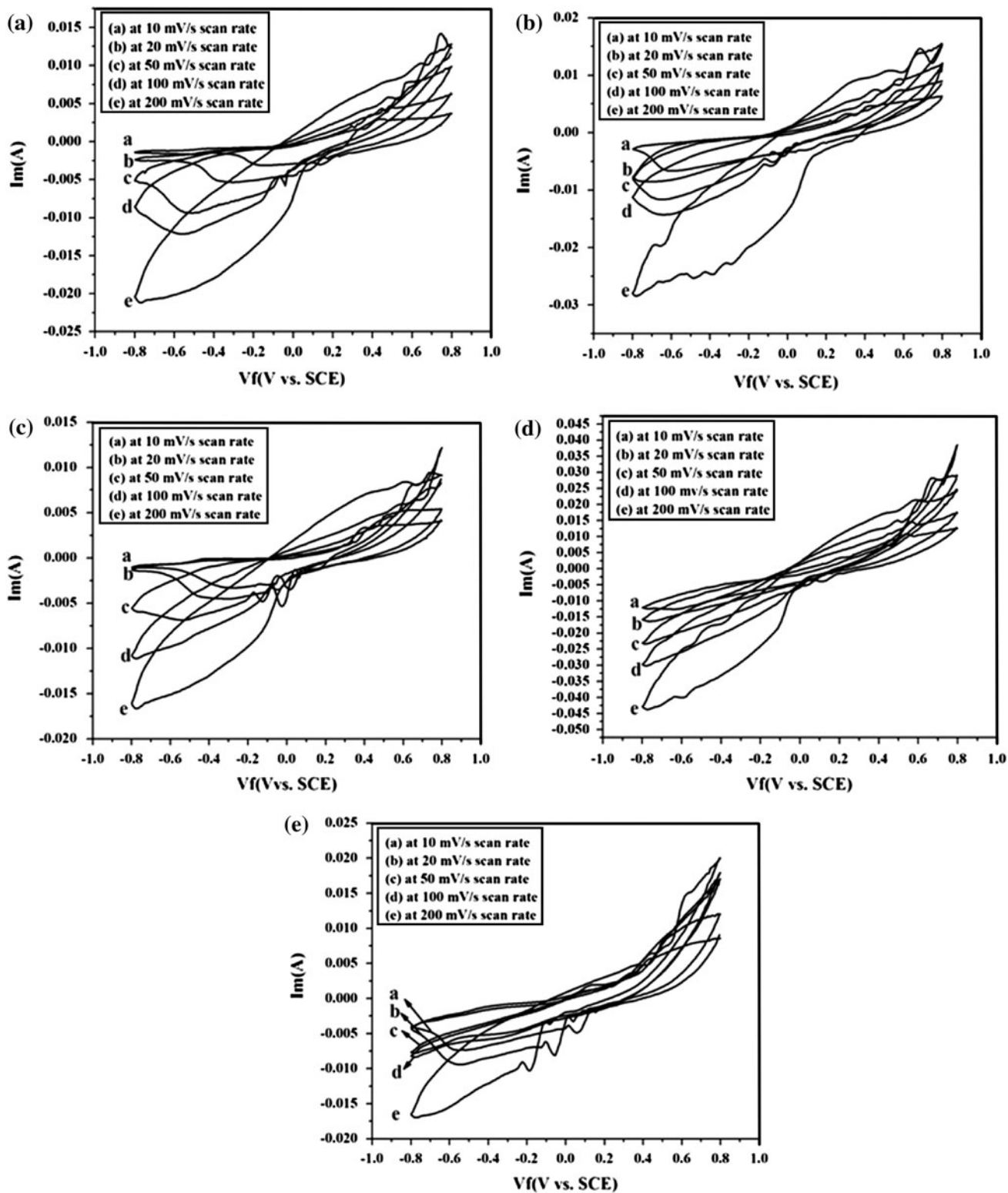Fig. 3 TEM image of **a** PANI C1, and **b** PANI C2 composites

Fig. 4 CV curves at different scan rate of **a** pure PANI, **b** PANI C1, **c** PANI C2, **d** PANI C3, and **e** PANI C4 composites

supercapacitors is their low energy density. In this present work, the entire PANI doped CuCl₂ composites along with PANI show better energy density as well as power density.

The energy densities of the PANI and PANI doped with CuCl₂ composites were calculated by the following equation:

Table 2 Specific capacitance of PANI and CuCl$_2$ doped PANI composites at different scan rate

Sample	10 mV/s	20 mV/s	50 mV/s	100 mV/s	200 mV/s
PANI	397	316	169	92	51
PANI C1	458	306	166	104	76
PANI C2	626	425	250	183	102
PANI C3	381	252	144	89	62
PANI C4	439	285	198	112	81
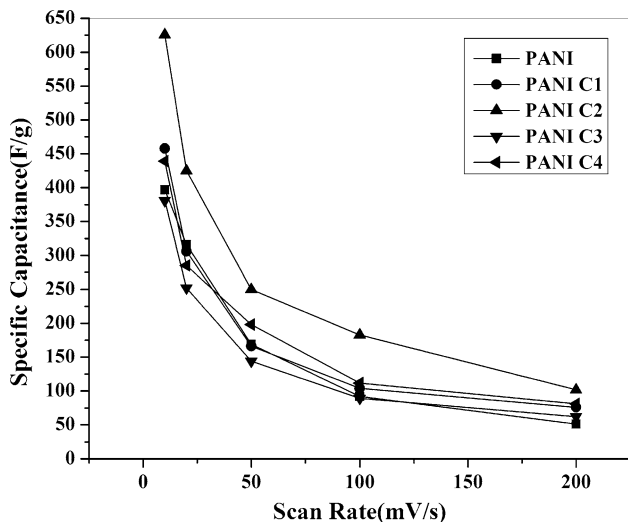
Fig. 5 Plot of specific capacitance versus scan rate of the pure PANI and PANI doped with CuCl$_2$ composites

Table 3 Energy density of PANI and CuCl$_2$ doped PANI composites at different scan rate

Sample	10 mV/s	20 mV/s	50 mV/s	100 mV/s	200 mV/s
PANI	141.15	112.35	60.08	31.71	18.13
PANI C1	162.84	108.8	59.02	36.97	27.02
PANI C2	222.57	151.11	88.88	65.06	36.26
PANI C3	135.46	89.6	51.2	31.64	22.04
PANI C4	156.08	101.33	70.4	39.46	28.8

Table 4 Power density of PANI and CuCl$_2$ doped PANI composites at different scan rate

Sample	10 mV/s	20 mV/s	50 mV/s	100 mV/s	200 mV/s
PANI	1,587.93	2,527.87	3,375	3,680	4,079.25
PANI C1	1,831.95	2,448	3,319.32	4,159.12	6,079.5
PANI C2	2,503.91	3,399.97	4,999.5	7,318.12	8,158.5
PANI C3	1,523.93	2,016	2,880	3,559.5	4,959
PANI C4	1,755.9	2,279.93	3,960	4,480	6,480

$$\text{Energy density } (E) = \tfrac{1}{2}(CV^2) \qquad (2)$$

where, C = specific capacitance in F/g, and V = operating voltage, where as power densities were calculated by the following equation:

$$\text{Power density } (P) = E/t \qquad (3)$$

where, t = time in second for complete cycle.

The energy densities of PANI and PANI doped CuCl$_2$ composites at various scan rates are given in Table 3. The highest energy density of 222.57 Wh/Kg is obtained for PANI C2 at 10 mV/s. The power density at different scan rate for PANI and PANI doped CuCl$_2$ composites are shown in Table 4. The highest energy density of 8,158.5 W/Kg is obtained for PANI C2 at 200 mV/s.

4.5 Electrochemical impedance spectroscopy

The most widely employed plot for the analysis of EIS data is Nyquist plot. The Nyquist plots are typically interpreted by fitting the experimental impedance spectra to an equivalent electrical circuit. The fitted Nyquist plot of the pure PANI and CuCl$_2$ doped PANI composites at 0 V are shown in Fig. 6. The region at higher frequencies represents the electrolyte properties, and the region in mid frequency is related with electrode/electrolyte interface processes. The corresponding relaxation effect is represented by a semicircle whose intersection at higher frequency and mid frequency with real axis is solution resistance (R$_s$) and charge transfer resistance (R$_{ct}$), respectively.

The suitable equivalent circuit stimulated to the experimental data is shown in Fig. 7 and the fitting dada of the PANI and PANI doped composites is summarized in Table 5. The equivalent circuit used here is the standard circuit for "CPE with diffusion" and already been used by several research group all over the world [44, 45]. In real-world systems, the capacitors are not ideal. These imperfect capacitors are represented as constant phase element (CPE), which are attributed by depressed semicircle in Nyquist plot. CPE may be arise from (a) distribution of relaxation times as a result of inhomogeneity at the electrode/electrolyte interface, (b) porosity, (c) the nature of the electrode, and (d) dynamic disorder associated with diffusion [38].

The solution resistance of 1.79, 1.7, 1.81, 1.56, and 1.72 Ω were obtained for PANI, PANI C1, PANI C2, PANI C3, and PANI C4 composites respectively. The charge transfer resistance and Warburg resistance (W) was found to be highest in PANI C2 due to maximum charge delocalization of Cu^{2+} ions in PANI C2 composite. The highest value of n $\sim$ 0.78 was obtained in PANI C2 composite which indicates the porous nature of the electrode. The lower solution resistance obtained from EIS measurements indicates the superior capacitive behavior.
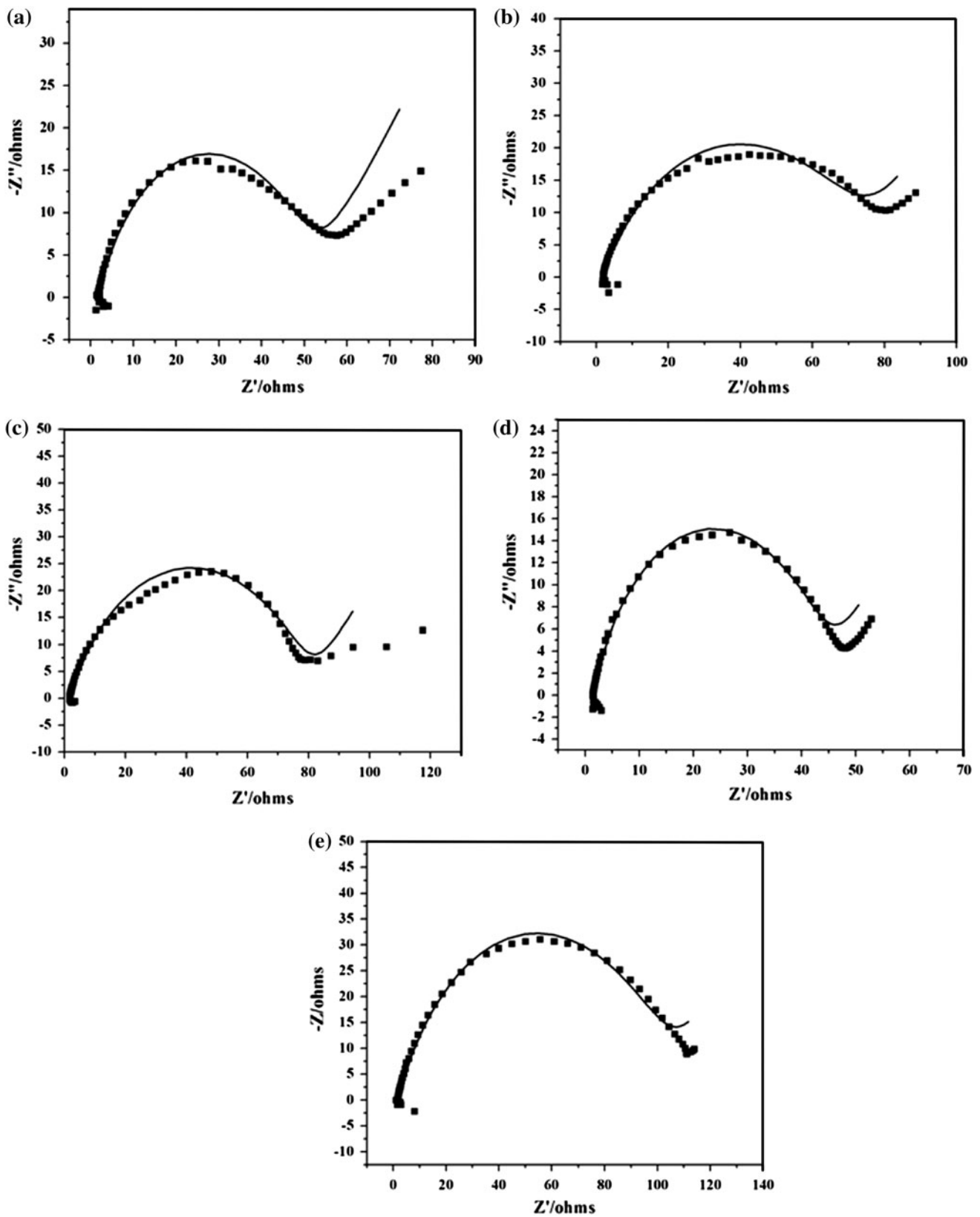
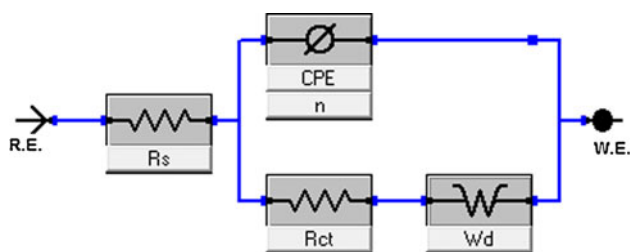**Fig. 6** Nyquist plot of **a** PANI, **b** PANI C1, **c** PANI C2, **d** PANI C3, and PANI C4

Fig. 7 Equivalent electrical circuit used in EIS fitting data

Table 5 Fitting data for equivalent electrical circuit elements of PANI composites and $CuCl_2$ doped PANI composites

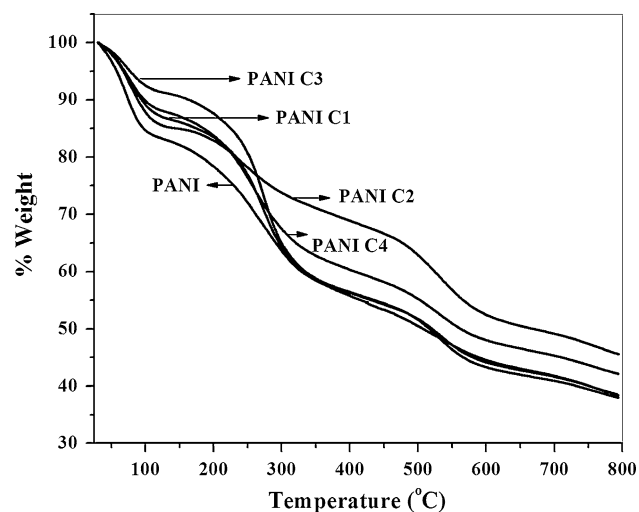| Sample	R_s (Ω)	R_{ct} (Ω)	W $(S-s^{0.5})$ $\times 10^{-2}$	CPE $(S-s^n)$ $\times 10^{-3}$	n
PANI	1.794	49.46	2.9	0.125	0.75
PANI C1	1.7	72.86	1.77	0.15	0.64
PANI C2	1.816	78.10	5.814	0.17	0.78
PANI C3	1.567	42.76	4.52	0.164	0.77
PANI C4	1.723	102.4	4.0	0.22	0.70

Fig. 8 TGA plot of PANI, PANI C1, PANI C2, PANI C3, and PANI C4 composites

4.6 TGA analysis

The effect of $CuCl_2$ doping percentages on thermal stability of the composites was analyzed by TGA and the plots are shown in Fig. 8. For all the composites, the initial weight loss was observed due to the removal of water molecules. For undoped PANI, 40 % weight loss was observed at around 300 °C. This second weight loss was observed due to the degradation of polymer chains. However, this 40 % weight loss was occurred at around 500 °C in PANI C2. This confirms the enhanced thermal stability of PANI C2 as compared to undoped PANI. On the other hand, the third weight loss at around 600 °C may be

Table 6 Thermal stability data of PANI and $CuCl_2$ doped PANI composites extracted from TGA plots

Sample	Weight loss at temperature (%)			
	100 °C	300 °C	500 °C	700 °C
PANI	15.18	36.41	49.64	58.23
PANI C1	10.83	35.7	48.59	59.18
PANI C2	12.19	26.29	36.92	50.78
PANI C3	7.56	35	48.32	58.39
PANI C4	10.28	32.41	44.88	54.59

observed due to the elimination of dopant molecules from the composites [31]. In Brief, form the TGA thermogram, it can be stated that PANI C2 achieved the maximum thermal stability at higher temperature ($\sim$300–800 °C) due to the maximum interaction of Cu^{2+} with PANI at 2 wt% doping level. The TGA values at different temperature regions are shown in Table 6.

5 Conclusion

We have investigated the electrochemical performance of Pseudocapacitor based on $CuCl_2$ doped PANI composites. The composites were synthesized by in situ oxidative polymerization method, using APS as oxidant in HCl medium. Among all the materials, PANI shows highest specific capacitance value of 626 F/g at 10 mV/s scan rate at 2 wt% doping level. The same electrode material also shows highest energy density (222.57 Wh/Kg at 10 mV/s scan rate) and power density (8,158.5 W/Kg at 200 mV/s scan rate). Moreover, this composite also have the highest thermal stability, among all the composites. However, PANI at 2 wt% doping level showed promising electrochemical properties. Further fabrication of the composites as well as experimental conditions will lead good application potential in supercapacitor as well as other device applications.

References

1. R. Menon, C.O. Yoon, D. Moses, A.J. Heeger, in *Handbook of Conducting Polymers*, 2nd edn, ed. by T.A. Skotheim, R.L. Elsenbaumer, J.R. Reynolds (Marcel Dekker, New York, NY, 1998)
2. A.B. Kaiser, Adv. Mater. **13**, 927 (2001)
3. R.S. Kohlman, J. Joo, A.J. Epstein, in *Physical Properties of Polymers Handbook*, ed. by J.E. Mark (AIP, New York, NY, 1996)
4. C. Fite, Y. Cao, A.J. Heeger, Solid State Commun. **73**, 607 (1990)

5. Y.W. Park, E.S. Choi, D.S. Suh, Synth. Met. **96**, 81 (1998)
6. P.N. Bartlett, P.R. Birkin, Synth. Met. **61**, 15 (1993)
7. J. Joo, A. Epstein, Appl. Phys. Lett. **65**, 2278 (1994)
8. J.A. Osaheni, A.S. Jenekhe, H. Vanherzeele, J.S. Meth, Y. Sun, A.G. MacDiarmid, J. Phys. Chem. **96**, 2830 (1992)
9. Z.-L. Hau, J.-L. Shi, L.-X. Zhang, M.-L. Ruan, J.-N. Yan, Adv. Mater. **14**, 830 (2002)
10. N. Asim, S. Radiman, M.A. Bin Yarmo, Mater. Lett. **62**, 1044 (2008)
11. P. Ghosh, A. Chakrabarti, S.K. Siddhanta, Eur. Polym. J. **35**, 803 (1999)
12. E.T. Kang, K.G. Neoh, K.L. Tan, Prog. Polym. Sci. **23**, 277 (1998)
13. M.K. Ram, S. Annapoorni, S.S. Pandey, B.D. Malhotra, Polymer **39**, 3399 (1998)
14. H.S. Kim, H.L. Hobbs, L. Wang, M.J. Rutten, C.C. Wamser, Synth. Met. **159**, 1313 (2009)
15. R. Singh, V. Arora, R.P. Tandon, A. Mansingh, S. Chandra, Synth. Met. **104**, 137 (1999)
16. E. Erdem, M. Karakisla, M. Sacak, Eur. Polym. J. **40**, 785 (2004)
17. N.J. Pinto, A.A. Acosta, G.P. Sinha, F.M. Aliev, Synth. Met. **113**, 77 (2000)
18. B.K. Sharma, A.K. Gupta, N. Khare, S.K. Dhawan, H.C. Gupta, Synth. Met. **159**, 391 (2009)
19. T. Hino, T. Namiki, N. Kuramoto, Synth. Met. **156**, 1327 (2006)
20. R.M.G. Rajapaske, D.M.M. Krishantha, D.T.B. Tennakoon, H.V.R. Dias, Electrochim. Acta **51**, 2483 (2006)
21. C.-H. Chen, J. Appl. Polym. Sci. **89**, 2142 (2003)
22. X. Li, X. Li, Mater. Lett. **61**, 2011 (2007)
23. R. Singh, V. Arora, R.P. Tandon, S. Chandra, J. Mater. Sci. **33**, 2067 (1998)
24. B.E. Conway, *Electrochemical Supercapacitors: Scientific, Fundamentals, and Technological Applications* (Kluwer, New York, NY, 1999)
25. R. Kötz, M. Carlen, Electrochim. Acta **45**, 2483 (2000)
26. E. Frackowiak, F. Béguin, Carbon **39**, 937 (2001)
27. T.C. Griija, M.V. Sangaranarayanan, J. Power Sources **156**, 705 (2006)
28. S. Palaniappan, A. John, C.A. Amarnath, V.J. Rao, J. Mol. Catal. A Chem. **218**, 47 (2004)
29. S. Sathiyanarayanan, C. Jeyaprabha, G. Venkatachari, Mater. Chem. Phys. **107**, 350 (2008)
30. E. Ozkazanc, S. Zor, H. Ozkazanc, Polym. Compos. **31**, 1862 (2010)
31. K. Gupta, G. Chakraborty, S. Ghatak, P.C. Jana, A.K. Meikap, J. Appl. Polym. Sci. **115**, 2911 (2010)
32. C. Yang, C. Chen, Synth. Met. **153**, 133 (2005)
33. B.L. Rivas, C.O. Sanchez, J. Appil, Polym. Sci. **82**, 330 (2001)
34. O.P. Dimitriev, Macromolecules **37**, 3388 (2004)
35. O.P. Dimitriev, Synth. Mat. **14**, 299 (2004)
36. M. Gizdavic-Nikolaidis, J. Travas-Sejdic, R.P. Cooney, G.A. Bowmaker, Curr. Appl. Phys. **6**, 457 (2006)
37. J. Li, M. Chi, Y. Lai, Z. Zhang, H. Lu, J. Fang, Y. Lie, Synth. Met. **160**, 1228 (2010)
38. D.S. Patil, J.S. Shaikh, D.S. Dalavi, M.M. Karanjkar, R.S. Devan, Y.R. Ma, P.S. Patil, J. Electrochem. Soc. **158**, A653 (2011)
39. K.S. Ryu, X. Wu, Y.G. Lee, S.H. Chang, J. Appl. Polym. Sci. **89**, 1300 (2003)
40. S. Palaniappan, S.L. Devi, J. Appl. Polym. Sci. **107**, 1887 (2008)
41. S. Sahoo, G. Karthikeyan, G.C. Nayak, C.K. Das, Synth. Met. **161**, 1713 (2011)
42. M. Moniruzzaman, C.K. Das, Macromol. Symp. **298**, 34 (2010)
43. J. Wang, Y.L. Xu, X.F. Sun, S.C. Mao, F. Xiao, J. Electrochem. Soc. **154**, C445 (2007)
44. J. Bisquert, G.G. Belmonte, P. Bueno, E. Longo, L.O.S. Bulhoes, J. Electroanal. Chem. **452**, 229 (1998)
45. V. Feliu, J.A. Gonzalez, C. Andrade, S. Feliu, Corros. Sci. **140**, 975 (1998)